

Higher-order Neural Additive Models: An Interpretable Machine Learning Model with Feature Interactions

Minkyu Kim,¹ Hyun-Soo Choi,² Jinho Kim²

¹ Clinical Decision Support Systems Team, Ziovision Inc., South Korea

² Department of Computer Science and Engineering, Kangwon National University, South Korea
minkyu.kim@ziovision.co.kr, choi.hyunsoo@kangwon.ac.kr, jhkim@kangwon.ac.kr

Abstract

Black-box models, such as deep neural networks, exhibit superior predictive performances, but understanding their behavior is notoriously difficult. Many explainable artificial intelligence methods have been proposed to reveal the decision-making processes of black box models. However, their applications in high-stakes domains remain limited. Recently proposed neural additive models (NAM) have achieved state-of-the-art interpretable machine learning. NAM can provide straightforward interpretations with slight performance sacrifices compared with multi-layer perceptron. However, NAM can only model 1st-order feature interactions; thus, it cannot capture the co-relationships between input features. To overcome this problem, we propose a novel interpretable machine learning method called higher-order neural additive models (HONAM) and a feature interaction method for high interpretability. HONAM can model arbitrary orders of feature interactions. Therefore, it can provide the high predictive performance and interpretability that high-stakes domains need. In addition, we propose a novel hidden unit to effectively learn sharp-shape functions. We conducted experiments using various real-world datasets to examine the effectiveness of HONAM. Furthermore, we demonstrate that HONAM can achieve fair AI with a slight performance sacrifice. The source code for HONAM is publicly available¹.

Introduction

Deep neural networks have achieved great success in various fields, such as computer vision and natural language processing. However, understanding and interpreting the decision processes of black-box models, such as neural networks, are notoriously difficult (Agarwal et al. 2020). Therefore, their application is limited to high-stakes domains, such as healthcare and social safety. Therefore, explainable artificial intelligence (AI) methods to explain the behaviors of black box models have been widely studied in recent years. Local interpretable model-agnostic explanations (LIME) (Ribeiro, Singh, and Guestrin 2016) is a representative explainable AI method. It attempts to locally approximate a black-box model using an interpretable model to explain individual predictions. LIME can explain a local area of the black-box model if the interpretable model has approximated the black-box model to be explained well. However, LIME often fails to explain the global behavior of

the black box model. Shapley additive explanation (SHAP) (Lundberg and Lee 2017) is a game-theoretic approach for model-agnostic explanations. SHAP generates predictions of a black-box model based on possible combinations of input features and obtains the effect of a feature by exploiting changes in predictions when the feature is dropped. However, the explanation of SHAP may not be faithful to the actual predictions of the black-box model. As mentioned above, explainable AI methods are still limited in their applications to high-stakes domains because they often fail to explain and may not be faithful to the actual behaviors of black-box models; thus, we need interpretable AI methods (Rudin 2019).

The recently proposed neural additive models (NAM) (Agarwal et al. 2020) are state-of-the-art methods of interpretable machine learning. Since NAM learns a linear combination of neural networks corresponding to each input feature, it can model nonlinear relationships between each input feature and the output. In addition, NAM can provide straightforward interpretations and has a predictive performance comparable to that of multi-layer perceptron (MLP) and tree-based methods, such as XGBoost (Chen and Guestrin 2016). However, NAM can only model 1st-order feature interactions. Therefore, NAM cannot capture the co-relationships between input features even though there are many such relationships in real-world data. More recently, (Chang, Caruana, and Goldenberg 2022) have proposed NodeGAM and NodeGA²M which are neural decision tree-based generalized additive models (GAMs). However, NodeGAM and NodeGA²M also merely can learn 1st-order and 2nd-order feature interactions, respectively. If there is an interpretable machine learning method that can model high-order feature interactions, it will not only provide high-quality interpretations, but also show better predictive performance.

Methods for explicitly modeling feature interactions using machine learning have been studied extensively (Rendle 2010; Cheng et al. 2016; Wang et al. 2017; Guo et al. 2017; Lian et al. 2018). Feature interaction methods aim to model high-order interactions through feature crossing, which iteratively multiplies input features, and has shown impressive performance in predictive tasks, such as recommendation (Lian et al. 2018) and regression (Kim, Lee, and Kim 2020). However, there are several problems with the

¹<https://github.com/gim485744/HONAM>

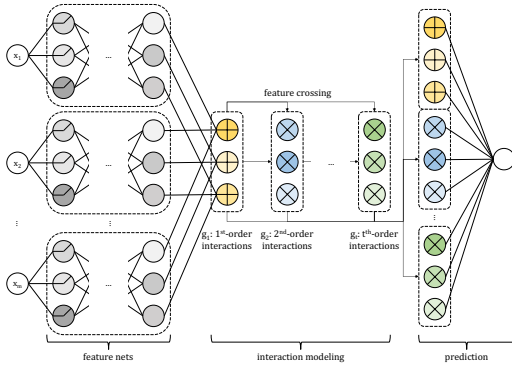


Figure 1: The Architecture of HONAM

existing feature interaction methods. First, explicit feature interaction methods are linear. Therefore, they cannot learn nonlinear functions, and their expressive powers are limited. Second, most existing feature interaction modeling studies have mainly focused on improving predictive performance. Although linear models are interpretable, their interpretability tends to be neglected in previous studies.

Since sharp jumps are frequently found in real-world data, making machine-learning models that can learn sharp jumps is a significant challenge in interpretable models (Agarwal et al. 2020; Chang et al. 2021). However, neural networks struggle to capture such sharp jumps (Agarwal et al. 2020) because of the bias towards smooth functions (Arpit et al. 2017; Rahaman et al. 2019). (Agarwal et al. 2020) have proposed the exp centered (ExU) unit to address this problem. However, the ExU unit merely works well under certain circumstances.

To overcome these problems, we propose a novel interpretable machine learning method called higher-order neural additive models (HONAM). Since HONAM learns a linear combination of neural networks corresponding to each input feature like NAM, it can not only effectively model nonlinear relationships between each input feature and the output, but is also still interpretable. The major difference between HONAM and NAM is that HONAM can model high-order feature interactions. It allows HONAM to capture the co-relationships between features and provides high-quality interpretations and better predictive performance than NAM. Furthermore, we propose a novel feature interaction modeling method for high interpretability because we may struggle to interpret the predictions of HONAM when using the existing feature interaction methods. We conduct extensive experiments to examine its effectiveness and demonstrate the interpretability of the HONAM. Experimental results demonstrate that HONAM has a higher or comparable predictive performance than MLP and XGBoost, even though it is an interpretable method and can provide high-quality interpretations. In addition, we propose a novel hidden unit named ExpDive to learn sharp shape functions, and we show that a trained HONAM can become a fair AI by removing biases.

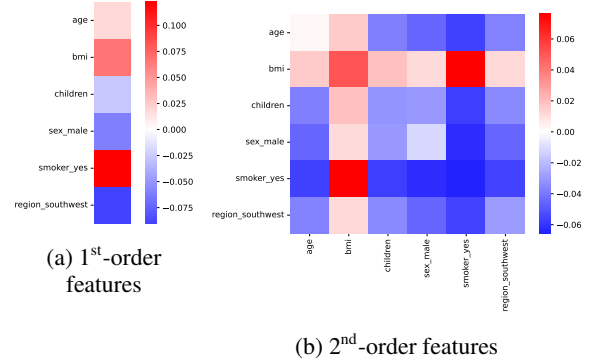


Figure 2: Feature contributions on the Insurance dataset learned by the CrossNet

Higher-order Neural Additive Models

In this section, we introduce HONAM, a novel interpretable machine-learning method that can model arbitrary orders of feature interactions. First, we describe NAM (Agarwal et al. 2020) and transform it to model feature interactions. We then present HONAM with element-wise feature crossing. Finally, we propose a novel feature interaction method for high interpretability and apply it to HONAM.

Transformation of Neural Additive Models

NAM learns a linear combination of MLPs corresponding to each feature. Accordingly, the computational result of each MLP indicates the direct effect of each feature on prediction. Owing to this characteristic, the interpretations of NAM are straightforward. In the original work, NAM was defined as follows:

$$\hat{y} = \sum_{i=1}^m f_i(x_i) + b, \quad (1)$$

where $x \in \mathbb{R}^m$ is the input feature, $f_i : \mathbb{R} \rightarrow \mathbb{R}$ is the MLP corresponding to the i^{th} feature, $b \in \mathbb{R}$ is the output bias, and m is the number of features. As shown in Equation 1, NAM is an extension of the generalized additive models (GAM) (Hastie and Tibshirani 1987). The outputs of all feature networks in NAM are scalars, but the outputs should be vectors to effectively model the feature interactions. Therefore, we transform NAM as follows:

$$\mathcal{F}(x) = \sum_{i=1}^m f_i(x_i), \quad (2)$$

where $f_i : \mathbb{R} \rightarrow \mathbb{R}^k$ is the MLP corresponding to the i^{th} feature, similar to the existing NAM, but the output is a k -dimensional vector. Since $\mathcal{F} : \mathbb{R}^m \rightarrow \mathbb{R}^k$ is a function that adds all representation vectors of the input features, the output of \mathcal{F} can be viewed as the sum of 1st-order features.

Modeling High-order Feature Interactions

A simple way to model high-order feature interactions is to enumerate all feature interactions (Rendle 2010) as follows:

$$g_t(x) = \sum_{i_1=1}^m \sum_{i_2=i_1+1}^m \dots \sum_{i_t=i_{t-1}+1}^m \prod_{l=1}^t x_{i_l}, \quad (3)$$

where t is the order of feature interactions we want to model. This method makes all possible combinations of t^{th} -order features using m features. Simply enumerating all possible interactions is intuitive. However, this method has $O(km^t)$ time complexity, which is exponential time; where k is the embedding size for x . Therefore, this method shows very slow training and inference times.

Another way to model feature interactions is to use multi-layer architecture (Wang et al. 2017) defined as follows:

$$g_t(x) = (g_1(x) \odot g_{t-1}(x)) W_t, \quad (4)$$

$$g_1(x) = xW_1, \quad (5)$$

where $W_1 \in \mathbb{R}^{m \times k}$ and $W_{t>1} \in \mathbb{R}^{k \times k}$ are the trainable weights. We refer to this method CrossNet. CrossNet multiplies $g_1(x)$ in every each layer to model high-order feature interactions. For example, the 1st layer $g_1(x) = xW_1$ indicates the weighted sum of 1st-order features. The 2nd layer $g_2(x) = (g_1(x) \odot g_1(x))W_2$ is the multiplication of two weighted sum of 1st-order features. In other words, it indicates the weighted sum of 2nd-order features. Its multi-layer structure is similar to MLP, but there is no activation function. Therefore, CrossNet is a linear model, and t -layer CrossNet can explicitly model t^{th} -order feature interactions. In addition, CrossNet has $O(tk^2)$ time complexity, which is significantly faster than the enumerating method.

However, CrossNet has problems from the interpretability perspective. CrossNet also models powers of features such as x_1^2 , x_2^2 , or $x_1x_2^2$. Such powers of features may confuse us in interpreting prediction results. For example, Figure 2a and Figures 2b show the heat maps of 1st-order and 2nd-order features' contribution values on the Insurance dataset learned by the CrossNet. In the 2nd-order features, human cannot know the meaning of squared features such as $(sex = male)^2$ and $(smoker = yes)^2$. Therefore, powers of features have no meaning from the interpretability perspective. In addition, 1st-order feature $(smoker = yes)$ has highly positive value, but squared feature $(smoker = yes)^2$ has negative value. As can be seen in Figure 2, powers of features can have different contributions with their 1st-order features. This phenomenon confuses people in determining the actual effect of $(smoker = yes)$.

Novel Feature Crossing for High Interpretability

We would like to make a novel feature interaction method, which is fast and powers of features are eliminated. To achieve this goal, we found a recursion form of the enumerating method.

Theorem 1 We develop a method for recursively eliminating powers of features. First, we make t^{th} -order features

with squared features as follows:

$$\left(\sum_{i=1}^m x_i \right) \left(\sum_{i_1 > \dots > i_{t-1}} \prod_{l=1}^{t-1} x_{i_l} \right). \quad (6)$$

Equation 6 indicates the multiplication of the sum of $(t-1)^{\text{th}}$ -order features and the sum of 1st-order features. Therefore, there are t^{th} -order features with squared features. To remove the squared features, we explicitly subtract them. However, unexpected features also eliminated in this process. Therefore, we repeat subtracting powers of features and adding back unexpectedly eliminated features as follows:

$$\begin{aligned} & \left(\sum_{i=1}^m x_i \right) \left(\sum_{i_1 > \dots > i_{t-1}} \prod_{l=1}^{t-1} x_{i_l} \right) \\ & - \left(\sum_{i=1}^m x_i^2 \right) \left(\sum_{i_1 > \dots > i_{t-2}} \prod_{l=1}^{t-2} x_{i_l} \right) \\ & + \left(\sum_{i=1}^m x_i^3 \right) \left(\sum_{i_1 > \dots > i_{t-3}} \prod_{l=1}^{t-3} x_{i_l} \right) \\ & - \dots \end{aligned} \quad (7)$$

Now, we can make this iteration to recursion form as follows:

$$g_t(x) = \frac{1}{t} \sum_{i=1}^t (-1)^{i+1} g_1(x^i) g_{t-i}(x), \quad (8)$$

$$g_1(x) = \sum_{i=1}^m x_i, \quad (9)$$

$$g_0(x) = 1. \quad (10)$$

Since, same interaction values are multiplied t times in Equation 7, we divide Equation 8 by t . Therefore, Equation 8 is equivalent to Equation 3, but our method has $O(ktm)$ time complexity, which is linear time when using dynamic programming. The proof of **Theorem 1** can be found in Appendix.

The final prediction process of HONAM is defined as follows:

$$\mathcal{G}(x) = \left(\parallel_{i=1}^t g_i(x) \right) W + b, \quad (11)$$

$$\hat{y} = \mathcal{G}(\mathcal{F}(x)), \quad (12)$$

where \parallel denotes the concatenation operator, W is the output weight, b is the output bias, \mathcal{G} is a feature interaction method such as our proposed method or CrossNet, and \mathcal{F} is the transformed NAM defined in Equation 2. Figure 1 shows the architecture of HONAM. We believe that our feature interaction method is a very useful choice for interpretable machine learning.

Relationship with Higher-order Factorization Machines

Although we started this study from a different perspective than HOFM (Blondel et al. 2016), our feature interaction method is equivalent to the alternative recursion form

| | California Housing | | Insurance | | House Prices | | Bikeshare | | Year | |
|-----------------------|------------------------------|------------------------------|------------------------------|------------------------------|------------------------------|------------------------------|------------------------------|------------------------------|------------------------------|------------------------------|
| | R-squared | R-absolute | R-squared | R-absolute | R-squared | R-absolute | R-squared | R-absolute | R-squared | R-absolute |
| LR | 0.630 (± 0.001) | 0.441 (± 0.002) | 0.780 (± 0.003) | 0.548 (± 0.014) | 0.830 (± 0.031) | 0.594 (± 0.036) | 0.362 (± 0.012) | 0.238 (± 0.012) | 0.247 (± 0.001) | 0.169 (± 0.001) |
| CrossNet (t=2) | 0.717 (± 0.001) | 0.525 (± 0.001) | 0.860 (± 0.005) | 0.688 (± 0.020) | 0.860 (± 0.057) | 0.655 (± 0.063) | 0.498 (± 0.008) | 0.316 (± 0.009) | 0.310 (± 0.001) | 0.211 (± 0.001) |
| XGBoost | 0.825 (± 0.001) | 0.649 (± 0.002) | 0.860 (± 0.009) | 0.735 (± 0.012) | 0.900 (± 0.016) | 0.711 (± 0.011) | 0.948 (± 0.003) | 0.816 (± 0.002) | 0.297 (± 0.000) | 0.201 (± 0.000) |
| MLP | 0.787 (± 0.005) | 0.614 (± 0.005) | 0.866 (± 0.002) | 0.711 (± 0.004) | 0.856 (± 0.026) | 0.688 (± 0.015) | 0.925 (± 0.006) | 0.762 (± 0.008) | 0.334 (± 0.003) | 0.247 (± 0.001) |
| EBM | 0.802 (± 0.001) | 0.612 (± 0.002) | 0.879 (± 0.002) | 0.736 (± 0.005) | 0.905 (± 0.006) | 0.726 (± 0.007) | 0.906 (± 0.003) | 0.737 (± 0.004) | 0.282 (± 0.001) | 0.191 (± 0.001) |
| NAM | 0.744 (± 0.002) | 0.549 (± 0.003) | 0.781 (± 0.003) | 0.544 (± 0.009) | 0.885 (± 0.013) | 0.715 (± 0.009) | 0.694 (± 0.006) | 0.476 (± 0.005) | 0.276 (± 0.001) | 0.185 (± 0.002) |
| NodeGAM | 0.734 (± 0.004) | 0.540 (± 0.004) | 0.776 (± 0.003) | 0.534 (± 0.004) | 0.897 (± 0.008) | 0.732 (± 0.007) | 0.696 (± 0.005) | 0.476 (± 0.005) | 0.275 (± 0.001) | 0.188 (± 0.001) |
| NodeGA ² M | 0.808 (± 0.004) | 0.620 (± 0.005) | 0.879 (± 0.004) | 0.732 (± 0.010) | 0.887 (± 0.015) | 0.712 (± 0.024) | 0.911 (± 0.004) | 0.740 (± 0.004) | 0.309 (± 0.001) | 0.213 (± 0.001) |
| HONAM* (t=2) | 0.807 (± 0.004) | 0.621 (± 0.004) | 0.880 (± 0.001) | 0.744 (± 0.003) | 0.900 (± 0.018) | 0.725 (± 0.017) | 0.920 (± 0.004) | 0.752 (± 0.008) | 0.320 (± 0.003) | 0.224 (± 0.003) |
| HONAM (t=2) | 0.810 (± 0.003) | 0.626 (± 0.003) | 0.882 (± 0.002) | 0.742 (± 0.012) | 0.900 (± 0.011) | 0.721 (± 0.009) | 0.925 (± 0.004) | 0.760 (± 0.006) | 0.320 (± 0.002) | 0.226 (± 0.004) |

Table 1: Evaluation on Regression Tasks

| | FICO | | Credit | | Support2 | | MIMIC III | | Click | |
|-----------------------|------------------------------|------------------------------|------------------------------|------------------------------|------------------------------|------------------------------|------------------------------|------------------------------|------------------------------|------------------------------|
| | AUROC | AUPRC | AUROC | AUPRC | AUROC | AUPRC | AUROC | AUPRC | AUROC | AUPRC |
| LR | 0.753 (± 0.001) | 0.723 (± 0.002) | 0.978 (± 0.012) | 0.800 (± 0.045) | 0.783 (± 0.009) | 0.577 (± 0.020) | 0.761 (± 0.012) | 0.317 (± 0.031) | 0.617 (± 0.002) | 0.620 (± 0.002) |
| CrossNet (t=2) | 0.770 (± 0.002) | 0.752 (± 0.004) | 0.964 (± 0.024) | 0.810 (± 0.038) | 0.803 (± 0.009) | 0.612 (± 0.013) | 0.787 (± 0.005) | 0.343 (± 0.022) | 0.619 (± 0.001) | 0.625 (± 0.001) |
| XGBoost | 0.767 (± 0.003) | 0.744 (± 0.004) | 0.980 (± 0.006) | 0.857 (± 0.035) | 0.800 (± 0.014) | 0.602 (± 0.018) | 0.791 (± 0.009) | 0.342 (± 0.025) | 0.687 (± 0.001) | 0.680 (± 0.001) |
| MLP | 0.770 (± 0.002) | 0.749 (± 0.003) | 0.980 (± 0.011) | 0.803 (± 0.051) | 0.801 (± 0.008) | 0.606 (± 0.013) | 0.792 (± 0.009) | 0.346 (± 0.025) | 0.627 (± 0.003) | 0.627 (± 0.002) |
| EBM | 0.700 (± 0.002) | 0.625 (± 0.002) | 0.885 (± 0.023) | 0.699 (± 0.048) | 0.674 (± 0.017) | 0.434 (± 0.019) | 0.563 (± 0.012) | 0.167 (± 0.017) | 0.592 (± 0.001) | 0.551 (± 0.001) |
| NAM | 0.783 (± 0.003) | 0.760 (± 0.003) | 0.979 (± 0.014) | 0.845 (± 0.036) | 0.815 (± 0.014) | 0.626 (± 0.011) | 0.815 (± 0.005) | 0.380 (± 0.025) | 0.655 (± 0.002) | 0.652 (± 0.002) |
| NodeGAM | 0.781 (± 0.002) | 0.761 (± 0.002) | 0.980 (± 0.012) | 0.849 (± 0.040) | 0.814 (± 0.012) | 0.626 (± 0.010) | 0.813 (± 0.006) | 0.375 (± 0.017) | 0.643 (± 0.002) | 0.643 (± 0.001) |
| NodeGA ² M | 0.780 (± 0.002) | 0.760 (± 0.003) | 0.982 (± 0.011) | 0.846 (± 0.038) | 0.812 (± 0.012) | 0.624 (± 0.008) | 0.816 (± 0.009) | 0.374 (± 0.023) | 0.641 (± 0.002) | 0.639 (± 0.002) |
| HONAM* (t=2) | 0.783 (± 0.003) | 0.761 (± 0.005) | 0.982 (± 0.009) | 0.842 (± 0.024) | 0.819 (± 0.009) | 0.633 (± 0.011) | 0.825 (± 0.003) | 0.395 (± 0.023) | 0.667 (± 0.004) | 0.663 (± 0.003) |
| HONAM (t=2) | 0.782 (± 0.002) | 0.760 (± 0.004) | 0.981 (± 0.012) | 0.838 (± 0.026) | 0.823 (± 0.011) | 0.640 (± 0.009) | 0.826 (± 0.005) | 0.399 (± 0.024) | 0.670 (± 0.002) | 0.664 (± 0.003) |

Table 2: Evaluation on Classification Tasks

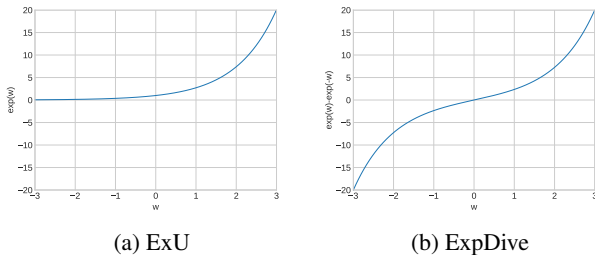


Figure 3: Weight shape functions of ExU and ExpDive units

of HOFM. Therefore, HOFM can be viewed as a special case of HONAM. Suppose that each feature network is linear, and the output weight is an all-one matrix. HONAM is equivalent to HOFM. Furthermore, HONAM overcomes the limitations of the existing FM/HOFM, feature interaction methods, and NAM. First, vanilla HOFM in the original work (Rendle 2010) has the time complexity of $O(km^t)$, but our feature interactions method has the time complexity of $O(tkm)$ when using dynamic programming as mentioned above; where k is the embedding size. Second, since FM/HOFM and other feature interaction methods are essentially linear models, their expressive powers are limited. HONAM can learn non-linear functions and has high expressive power because it utilizes neural networks, and is still interpretable. Third, NAM can only model 1st-order feature interactions, whereas HONAM can model high-order feature interactions. Thus, HONAM has higher predictive performance than NAM and can provide high-quality interpretations.

Learning Sharp Shape Functions

Since sharp jumps are frequently found in real-world data, making machine-learning models that can learn sharp jumps

is a significant challenge in interpretable models (Agarwal et al. 2020; Chang et al. 2021). For example, (Agarwal et al. 2020) found that the average house prices highly jump in San Francisco and Los Angeles in the California Housing dataset. In addition, (Chang et al. 2021) found that patients’ mortality risks significantly dropped at $PFRatio=332$ because they imputed missing values by the mean 332 (healthy patients commonly do not check PFRatio). However, neural networks struggle to capture such sharp jumps (Agarwal et al. 2020) because of the bias towards smooth functions (Arpit et al. 2017; Rahaman et al. 2019).

To address this problem, NAM uses the Exp Centered (ExU) unit defined as follows:

$$\sigma((x - b) \times \exp(W)). \quad (13)$$

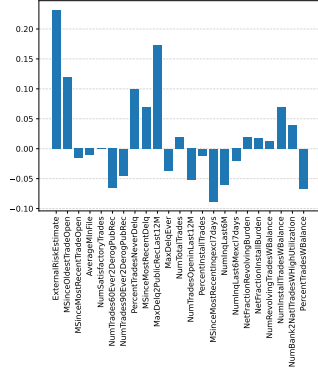
where σ is the ReLU-n function, x is the input feature, and W and b are the trainable weight and bias, respectively. The ExU unit can learn sharp jumps because its outputs are significantly changed with small input changes. However, the ExU unit works well under certain circumstances. In this section, we argue the limitations of the ExU unit and propose a novel hidden unit named the ExpDive unit, which is a more effective way to learn sharp shape functions.

Theorem 2 Since $\exp(W)$ is always positive, the ExU unit does not perform well when an input feature is negative. Suppose an ExU unit with ReLU activation, which is the bias term omitted, is as follows:

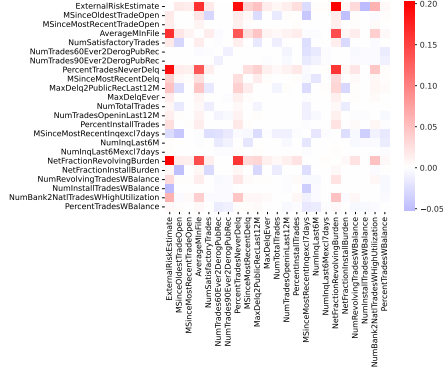
$$ReLU(x \times \exp(W)). \quad (14)$$

Equation 14 is always zero when x is negative. In other words, the gradient for the back-propagation is zero. Therefore, to propagate the gradient when x is negative, the bias b must be a negative number less than x . Therefore, the ExU unit often fails to learn. The proof of *Theorem 2* can be found in Appendix .

To overcome this problem, we propose the ExpDive unit. Since the ExpDive unit exponentially diverges in both the

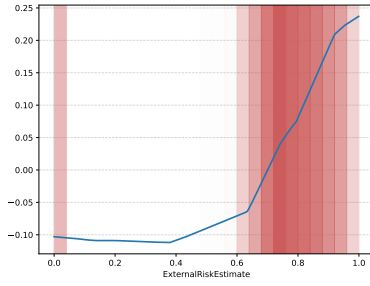


(a) Effects of first-order features

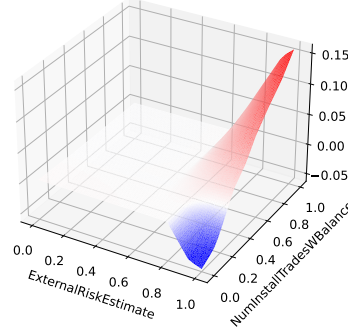


(b) Effects of second-order features

Figure 4: Local interpretations for the FICO dataset



(a) Effects of a first-order feature



(b) Effects of a second-order feature

Figure 5: Global interpretations for the FICO dataset

negative and positive ranges, it is not only suitable for learning sharp shape functions, but also the gradient vanishing problem does not occur. The ExpDive unit is defined as follows:

$$\sigma((x - b) \times (\exp(W) - \exp(-W))). \quad (15)$$

Figure 3 shows the shape plots of the weights of the ExU and ExpDive units. Contrary to the ExU unit, the ExpDive unit can propagate gradients if the weight is negative, even if the input x is negative.

Experiments

We conduct extensive experiments to demonstrate the effectiveness of HONAM. In addition, we conduct experiments to learn about sharp jumps and fair AI. Descriptions of the experimental setup and datasets is provided in Appendix.

Effectiveness of Modeling Feature Interactions

Although we mainly focus on the interpretability of HONAM in this study, we intend to show that feature interaction modeling is also effective for predictive performance. To this end, we compare HONAM with other machine-learning models using various regression and classification

datasets. Table 1 and Table 2 show the performance of the different comparative models on the regression and classification tasks, respectively. *HONAM** indicates HONAM with CrossNet, and *HONAM* indicates HONAM with the proposed interaction method in the tables. HONAM significantly outperforms EBM, NAM and NodeGAM in both regression and classification tasks. It shows that feature interaction modeling is effective for improving predictive performances. HONAM also outperforms NodeGA²M. It demonstrates that the fully neural network method (HONAM) is more effective than the tree-based method (NodeGAM). In addition, our HONAM outperforms or has comparable performances to full-complexity methods, MLP and XGBoost. Some GAM-based methods show better performance than MLP in several datasets. This may be because the distributions of each feature were different. Dealing with features with different distributions using shared trainable parameters may disturb training (Yan et al. 2022). Because NAM-family methods deal with features using different trainable parameters, this problem is alleviated. We also conduct an interaction ablation study in Appendix.

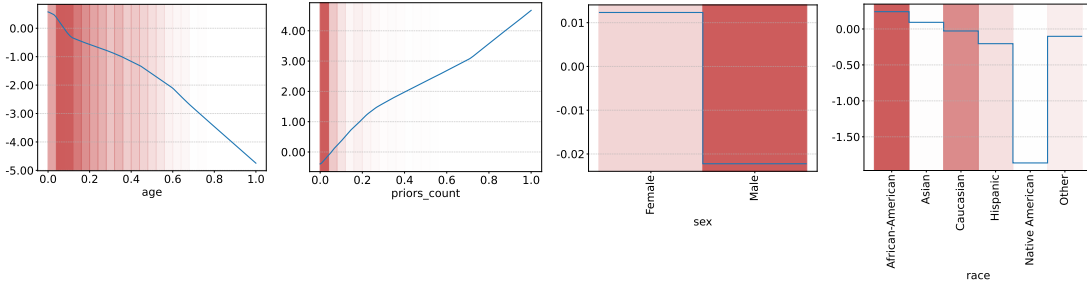


Figure 6: Learned shape functions on the COMPAS dataset

Interpretations

In HONAM, since each input feature is handled independently by the corresponding network, the computational result of each feature network indicates the direct effect of a feature on the output value. Owing to this characteristic, it is easy to interpret the predictions of HONAM. We can acquire local interpretations by forward propagation, and by repeating the process of local interpretation, we can also acquire global interpretations of HONAM. In this study, we visualize local interpretations of the 1st-order and 2nd-order features and visualize global interpretations to understand the global behavior of HONAM. Note that interpretations of high-order features, such as the 3rd-order or 4th-order, can also be obtained using HONAM.

Figure 4a and Figure 4b show the visualization of the local interpretations for the 1st-order and 2nd-order features in the FICO dataset, respectively. The figures show the actual contribution values of features to the prediction. We can get these values via the forward propagation of HONAM. For a more detailed explanation, we refer the representation vectors of each input feature x_1, x_2, \dots, x_m computed by the feature networks as r_1, r_2, \dots, r_m , where m is the number of features. To obtain 1st-order interpretation, the contribution value of feature i is computed by $r_i \times w_{0:k}$, where w is the output matrix and k is the size of the representation vector. Similarly, the contribution value of 2nd-order feature $(x_i * x_j)$ can be computed as $(r_i * r_j) \times w_{k:2*k}$. Because the FICO dataset is a binary classification task, features with positive effects increase the probability that the model predicts this data sample as positive, whereas features with negative effects decrease the probability. For a straightforward understanding, we visualize the interpretation of the 2nd-order features using a heat map. In Figure 4b, red cells indicate positive features, and blue cells indicate negative features.

In addition, we visualize the global interpretation of HONAM. Figure 5a and Figure 5b show the global interpretation of 1st-order feature *ExternalRiskEstimate* and 2nd-order feature *ExternalRistEstimate* \times *NumInstallTradesWBalance* in the FICO dataset, respectively. In Figure 5a, the red bars indicate the densities of training samples. In the 1st-order interpretation, *ExternalRistEstimate* tends to

| | AUROC | AUPRC |
|------------------------------------|-----------------------|-----------------------|
| HONAM | 0.832 (± 0.001) | 0.798 (± 0.001) |
| HONAM (remove sex bias) | 0.829 (± 0.001) | 0.794 (± 0.001) |
| HONAM (remove race bias) | 0.817 (± 0.002) | 0.787 (± 0.001) |
| HONAM (remove sex and race biases) | 0.816 (± 0.001) | 0.784 (± 0.002) |

Table 3: Predictive performances of biased and unbiased HONAMs

| African American vs | Overall | Asian | Caucasian | Hispanic | Native American | Other |
|---------------------|--------------|--------------|--------------|--------------|-----------------|--------------|
| HONAM | 0.349 | 0.327 | 0.398 | 0.293 | 0.358 | 0.174 |
| Unbiased HONAM | 0.524 | 0.383 | 0.547 | 0.458 | 0.823 | 0.502 |

Table 4: Disparate Impact on Race Features

have a more positive effect as increases. However, the 2nd-order interpretation exhibits a different tendency. In the 2nd-order interpretation, even if *ExternalRistEstimate* has a high value, it has a negative effect if *NumInstallTradesWBalance* is small. This is interesting because this tendency cannot be found in 1st-order interactions and can only be found in 2nd-order interactions. This demonstrates that HONAM can provide more detailed interpretations than NAM and why modeling high-order feature interaction is important in interpretable machine learning.

HONAM for Fair AI

Recently, fair AI has also attracted attention as a crucial machine learning research topic. Real-world datasets may have unexpected biases, and many researchers are working hard to eliminate such biases in machine-learning models. Fortunately, owing to the modularity of NAM (Agarwal et al. 2020), removing biases from trained HONAM is easy. We show that a HONAM trained on the COMPAS recidivism dataset is biased and introduce a method for eliminating biases.

Figure 6 shows the visualizations of the feature shape plots learned by HONAM for the COMPAS dataset. As shown in the figure, the trained HONAM is highly biased towards *race* features. These biases are undesirable and may be ethically problematic. Since HONAM handles each feature independently, it is easy to remove these biases. For example, we can drop out all feature networks correspond-

| | California Housing | | Insurance | | House Prices | |
|--------------------------|------------------------------|------------------------------|------------------------------|------------------------------|------------------------------|------------------------------|
| | Adj R-squared | Adj R-absolute | Adj R-squared | Adj R-absolute | Adj R-squared | Adj R-absolute |
| HONAM _{ExU} | 0.782 (± 0.011) | 0.594 (± 0.015) | 0.878 (± 0.004) | 0.735 (± 0.018) | 0.847 (± 0.023) | 0.613 (± 0.037) |
| HONAM _{ExpDive} | 0.797 (± 0.012) | 0.612 (± 0.015) | 0.878 (± 0.004) | 0.727 (± 0.016) | 0.850 (± 0.026) | 0.630 (± 0.022) |

Table 5: Predictive performance comparison of different units on regression tasks

| | FICO | | Credit | | MIMIC IV | |
|--------------------------|------------------------------|------------------------------|------------------------------|------------------------------|------------------------------|------------------------------|
| | AUROC | AUPRC | AUROC | AUPRC | AUROC | AUPRC |
| HONAM _{ExU} | 0.776 (± 0.006) | 0.756 (± 0.009) | 0.973 (± 0.005) | 0.842 (± 0.019) | 0.823 (± 0.001) | 0.074 (± 0.002) |
| HONAM _{ExpDive} | 0.780 (± 0.004) | 0.762 (± 0.006) | 0.975 (± 0.006) | 0.849 (± 0.014) | 0.823 (± 0.001) | 0.074 (± 0.001) |

Table 6: Predictive performance comparison of different units on classification tasks

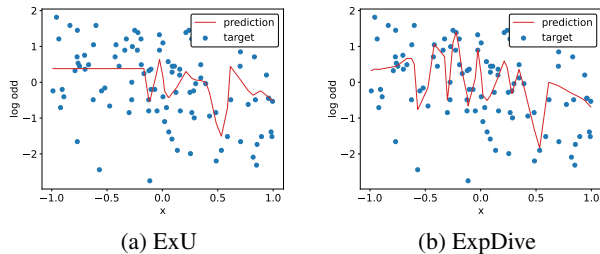


Figure 7: Learned shape functions of different units on the synthetic classification task

ing to race features to eliminate racial bias from the trained HONAM. Consequently, the effect of the *race* field is set to 0. Therefore, we can make a fair HONAM by sacrificing a slight predictive performance through this strategy, as shown in Table 3, which shows the predictive performance of biased and unbiased HONAMs. In addition, Table 4 shows the disparate impacts on race features for biased and unbiased HONAMs. The disparate impacts are significantly improved on all race features.

Comparison of Different Units

In this section, we demonstrate that the proposed ExpDive unit is more effective in learning sharp shape functions than the ExU unit using the synthetic classification dataset. Subsequently, we compare ExU, and ExpDive units to determine whether these units work well on real-world datasets.

Figure 7 shows the visualization of the feature shape plots learned by each unit for the synthetic classification dataset. Consistent with our theory, the ExU unit was not properly trained in the negative range. In addition, we can observe that the ExpDive unit trained the sharpest function on the dataset. The process of creating the synthetic dataset is described in Appendix, and more information on the experiment is also provided in Appendix.

Table 5 and Table 6 show the predictive performance of HONAMs with different units. The ExpDive unit outperforms the ExU unit. It demonstrates that our ExpDive unit is more effective than the ExU unit. We anticipate that the ExpDive unit will work well in fields where sharp jumps frequently occur, such as stock price predictions.

Conclusion

In this study, we proposed HONAM, a novel interpretable machine learning method that can model arbitrary orders of feature interactions. To develop the HONAM, we re-defined the existing NAM and applied CrossNet to model high-order feature interactions. Furthermore, we proposed a novel feature interaction method for high interpretability. We also proposed the ExpDive unit, which overcomes the limitations of the ExU unit, to effectively learn sharp shape functions. We conducted extensive experiments to examine the effectiveness of HONAM. The experimental results demonstrated that feature interaction modeling is effective for enhancing predictive performance, and HONAM outperforms or has comparable performance to MLP and XGBoost. We visualized both the local and global interpretations of HONAM for the 1st-order and 2nd-order features. These interpretations have shown that it is important to model high-order feature interactions in terms of interpretability, and HONAM can capture high-order correlations that NAM cannot. In addition, we showed that it is possible to create a fair HONAM by eliminating the biases of HONAM. HONAM has achieved high-performance interpretable machine-learning models required by high-stakes domains. We expect HONAM to be widely used in various domains, such as healthcare and mortality prediction.

References

- Agarwal, R.; Melnick, L.; Frosst, N.; Zhang, X.; Lengerich, B.; Caruana, R.; and Hinton, G. 2020. Neural Additive Models: Interpretable Machine Learning with Neural Nets. In *Proceedings of the 34th International Conference on Neural Information Processing Systems*.
- Arık, S. O.; and Pfister, T. 2021. TabNet: Attentive Interpretable Tabular Learning. In *AAAI*.
- Arpit, D.; Jastrzebski, S.; Ballas, N.; Krueger, D.; Bengio, E.; Kanwal, M. S.; Maharaj, T.; Fischer, A.; Courville, A.; Bengio, Y.; et al. 2017. A Closer Look at Memorization in Deep Networks. In *International conference on machine learning*.
- Blondel, M.; Fujino, A.; Ueda, N.; and Ishihata, M. 2016. Higher-Order Factorization Machines. In *Proceedings of the 29th International Conference on Neural Information Processing Systems*.

- Caruana, R. 1997. Multitask Learning. *Machine learning*, 28: 41–75.
- Caruana, R.; Lou, Y.; Gehrke, J.; Koch, P.; Sturm, M.; and Elhadad, N. 2015. Intelligible Models for HealthCare: Predicting Pneumonia Risk and Hospital 30-day Readmission. In *Proceedings of the 21th ACM SIGKDD international conference on knowledge discovery and data mining*.
- Chang, C.-H.; Caruana, R.; and Goldenberg, A. 2022. NODE-GAM: Neural Generalized Additive Model for Interpretable Deep Learning. In *International Conference on Learning Representations*.
- Chang, C.-H.; Tan, S.; Lengerich, B.; Goldenberg, A.; and Caruana, R. 2021. How Interpretable and Trustworthy are GAMs? In *Proceedings of the 27th ACM SIGKDD Conference on Knowledge Discovery & Data Mining*.
- Chen, T.; and Guestrin, C. 2016. XGBoost: A Scalable Tree Boosting System. In *Proceedings of the 22nd ACM SIGKDD International Conference on Knowledge Discovery and Data Mining*.
- Cheng, H.-T.; Koc, L.; Harmsen, J.; Shaked, T.; Chandra, T.; Aradhye, H.; Anderson, G.; Corrado, G.; Chai, W.; Ispir, M.; et al. 2016. Wide & Deep Learning for Recommender Systems. In *Proceedings of the 1st Workshop on Deep Learning for Recommender Systems*.
- Cheng, W.; Shen, Y.; and Huang, L. 2020. Adaptive Factorization Network: Learning Adaptive-Order Feature Interactions. In *Proceedings of the AAAI Conference on Artificial Intelligence*.
- Dal Pozzolo, A. 2015. Adaptive Machine Learning for Credit Card Fraud Detection. *PhD Thesis, Université libre de Bruxelles*.
- Guo, H.; Tang, R.; Ye, Y.; Li, Z.; and He, X. 2017. DeepFM: A Factorization-Machine Based Neural Network for CTR Prediction. In *Proceedings of the 26th International Joint Conference on Artificial Intelligence*.
- Hastie, T.; and Tibshirani, R. 1987. Generalized Additive Models: Some Applications. *Journal of the American Statistical Association*, 82: 371–386.
- Johnson, A.; Bulgarelli, L.; Pollard, T.; Horng, S.; Celi, L. A.; and Mark, R. 2021. MIMIC-IV. *PhysioNet*. <https://doi.org/10.13026/s6n6-xd98>.
- Johnson, A. E.; Pollard, T. J.; Shen, L.; Lehman, L.-w. H.; Feng, M.; Ghassemi, M.; Moody, B.; Szolovits, P.; Anthony Celi, L.; and Mark, R. G. 2016. MIMIC-III, A Freely Accessible Critical Care Database. *Scientific data*, 3(1): 1–9.
- Kim, M.; Choi, H.-S.; and Kim, J. 2022. Explicit Feature Interaction-aware Graph Neural Networks. *arXiv preprint arXiv:2204.03225*.
- Kim, M.; Lee, S.; and Kim, J. 2020. Combining Multiple Implicit-Explicit Interactions for Regression Analysis. In *2020 IEEE International Conference on Big Data (Big Data)*.
- Lian, J.; Zhou, X.; Zhang, F.; Chen, Z.; Xie, X.; and Sun, G. 2018. xDeepFM: Combining Explicit and Implicit Feature Interactions for Recommender Systems. In *Proceedings of the 24th ACM SIGKDD International Conference on Knowledge Discovery & Data Mining*.
- Lou, Y.; Caruana, R.; and Gehrke, J. 2012. Intelligible Models for Classification and Regression. In *Proceedings of the 18th ACM SIGKDD International Conference on Knowledge Discovery and Data Mining*.
- Lou, Y.; Caruana, R.; Gehrke, J.; and Hooker, G. 2013. Accurate Intelligible Models with Pairwise Interactions. In *Proceedings of the 19th ACM SIGKDD International Conference on Knowledge Discovery and Data Mining*.
- Lundberg, S. M.; and Lee, S.-I. 2017. A Unified Approach to Interpreting Model Predictions. In *Proceedings of the 30th International Conference on Neural Information Processing Systems*.
- Nori, H.; Jenkins, S.; Koch, P.; and Caruana, R. 2019. InterpretML: A Unified Framework for Machine Learning Interpretability. *arXiv preprint arXiv:1909.09223*.
- Popov, S.; Morozov, S.; and Babenko, A. 2019. Neural Oblivious Decision Ensembles for Deep Learning on Tabular Data. *arXiv preprint arXiv:1909.06312*.
- Potts, W. J. 1999. Generalized Additive Neural Networks. In *Proceedings of the fifth ACM SIGKDD international conference on Knowledge discovery and data mining*.
- Rahaman, N.; Baratin, A.; Arpit, D.; Draxler, F.; Lin, M.; Hamprecht, F.; Bengio, Y.; and Courville, A. 2019. On the Spectral Bias of Neural Networks. In *International Conference on Machine Learning*.
- Rendle, S. 2010. Factorization Machines. In *2010 IEEE International Conference on Data Mining*.
- Ribeiro, M. T.; Singh, S.; and Guestrin, C. 2016. "Why Should I Trust You?" Explaining the Predictions of Any Classifier. In *Proceedings of the 22nd ACM SIGKDD International Conference on Knowledge Discovery and Data Mining*.
- Rudin, C. 2019. Stop explaining black box machine learning models for high stakes decisions and use interpretable models instead. *Nature Machine Intelligence*, 1: 206–215.
- Wang, R.; Fu, B.; Fu, G.; and Wang, M. 2017. Deep & Cross Network for Ad Click Predictions. In *Proceedings of the ADKDD'17*.
- Xiao, J.; Ye, H.; He, X.; Zhang, H.; Wu, F.; and Chua, T.-S. 2017. Attentional Factorization Machines: Learning the Weight of Feature Interactions via Attention Networks. In *Proceedings of the 26th International Joint Conference on Artificial Intelligence*.
- Yan, B.; Wang, P.; Zhang, K.; Li, F.; Xu, J.; and Zheng, B. 2022. APG: Adaptive Parameter Generation Network for Click-Through Rate Prediction. *arXiv preprint arXiv:2203.16218*.

Proof of Theorem 1

We prove *Theorem 1* using mathematical induction.

Definition A.1. The sum of 1st-order feature interactions in which powers of features are completely removed can be defined as follows:

$$\begin{aligned} \sum_{i_1=1}^m \sum_{i_2=i_1+1}^m \cdots \sum_{i_t=t_{t-1}+1}^m \prod_{l=1}^t x_{i_l} \\ =: \sum_{i_1 > \dots > i_t} \prod_{l=1}^t x_{i_l}. \end{aligned}$$

Therefore, the proof must satisfy *Definition A.1*.

Lemma A.2. When the interaction order $t = 2$, *Theorem 1* is as follows:

$$\begin{aligned} g_2(x) &= \frac{1}{2} \sum_{i=1}^2 (-1)^{i+1} g_1(x^i) g_{2-i}(x) \\ &= \frac{1}{2} \{g_1(x) g_1(x) - g_1(x^2) g_0(x)\} \\ &= \frac{1}{2} \left\{ \left(\sum_{i=1}^m x_i \right) \left(\sum_{i=1}^m x_i \right) - \sum_{i=1}^m x_i^2 \right\} \\ &= \sum_{i_1=1}^m \sum_{i_2=i}^m x_{i_1} x_{i_2}. \end{aligned}$$

Therefore, *Theorem 1* holds when $t = 2$ because *Lemma A.1* satisfies *Definition A.1*.

Assumption A.3. Then, we assume that *Theorem 1* is true when $t = k - 1$ as follows:

$$\begin{aligned} g_{k-1}(x) &= \frac{1}{k-1} \sum_{i=1}^{k-1} (-1)^{i+1} g_1(x^i) g_{k-i-1}(x) \\ &= \sum_{i_1 > \dots > i_{k-1}} \prod_{l=1}^{k-1} x_{i_l}. \end{aligned}$$

Proof A.4. The sum of k^{th} -order interactions that include

powers of features is defined as follows:

$$\begin{aligned} \left(\sum_{i=1}^m x_i \right) \left(\sum_{i_1 > \dots > i_{k-1}} \prod_{l=1}^{k-1} x_{i_l} \right) \\ = k \sum_{i_1 > \dots > i_k} \prod_{l=1}^k x_{i_l} + \sum_{i=1}^m x_i^2 \sum_{\substack{j_1 > \dots > j_{k-1} \\ i \neq j_*}} \prod_{l=1}^{k-1} x_{j_l} \\ = k \sum_{i_1 > \dots > i_k} \prod_{l=1}^k x_{i_l} + \left(\sum_{i=1}^m x_i^2 \right) \left(\sum_{j_1 > \dots > j_{k-1}} \prod_{l=1}^{k-1} x_{j_l} \right) \\ - \sum_{i=1}^m x_i^3 \sum_{\substack{j_1 > \dots > j_{k-2} \\ i \neq j_*}} \prod_{l=1}^{k-2} x_{j_l} \\ = k \sum_{i_1 > \dots > i_k} \prod_{l=1}^k x_{i_l} + \left(\sum_{i=1}^m x_i^2 \right) \left(\sum_{j_1 > \dots > j_{k-1}} \prod_{l=1}^{k-1} x_{j_l} \right) \\ - \left(\sum_{i=1}^m x_i^3 \right) \left(\sum_{j_1 > \dots > j_{k-2}} \prod_{l=1}^{k-2} x_{j_l} \right) + \dots \\ = k \sum_{i_1 > \dots > i_k} \prod_{l=1}^k x_{i_l} \\ + \sum_{i=1}^{k-1} (-1)^{i+1} \left(\sum_{j=1}^m x_j^i \right) \left(\sum_{j_1 > \dots > j_{k-i}} \prod_{l=1}^{k-i} x_{j_l} \right). \end{aligned}$$

Therefore, eliminating powers of features from the above equation can be defined as follows:

$$\begin{aligned} \left(\sum_{i=1}^m x_i \right) \left(\sum_{i_1 > \dots > i_{k-1}} \prod_{l=1}^{k-1} x_{i_l} \right) \\ - \sum_{i=1}^{k-1} (-1)^{i+1} \left(\sum_{j=1}^m x_j^i \right) \left(\sum_{j_1 > \dots > j_{k-i}} \prod_{l=1}^{k-i} x_{j_l} \right) \\ = \sum_{i=1}^k (-1)^{i+1} \left(\sum_{j=1}^m x_j^i \right) \left(\sum_{j_1 > \dots > j_{k-i}} \prod_{l=1}^{k-i} x_{i_l} \right) \\ = k \sum_{i_1 > \dots > i_k} \prod_{l=1}^k x_{i_l}. \end{aligned}$$

Subsequently, we remove duplicated interactions by dividing k as follows:

$$\begin{aligned} \sum_{i_1 > \dots > i_k} \prod_{l=1}^k x_{i_l} \\ = \frac{1}{k} \sum_{i=1}^k (-1)^{i+1} \left(\sum_{j=1}^m x_j^i \right) \left(\sum_{j_1 > \dots > j_{k-i}} \prod_{l=1}^{k-i} x_{i_l} \right). \end{aligned}$$

Finally, we can obtain the recursion form of interactions by using *Lemma A.2* and *Assumption A.3* as follows:

$$\begin{aligned}
& \sum_{i_1 > \dots > i_k} \prod_{l=1}^k x_{i_l} \\
&= \frac{1}{k} \sum_{i=1}^k (-1)^{i+1} \binom{m}{j=1}^i x_j^i \binom{m}{j_1 > \dots > j_{k-i}}^{k-i} \prod_{l=1}^{k-i} x_{i_l} \\
&= \frac{1}{k} \sum_{i=1}^k (-1)^{i+1} g_1(x^i) g_{k-i}(x).
\end{aligned}$$

Consequently, *Theorem 1* is true because it satisfies *Definition A.1*. \square

Proof of Theorem 2

ExU units often fail to learn when using the ReLU activation, as shown below. The w with an exponential function always greater than zero as follows:

$$\forall w \in \mathbb{R} : \exp(w) > 0.$$

Therefore, the state of an ExU unit with the ReLU activation can be expressed as follows:

$$ReLU(x \times \exp(w)) = \begin{cases} x \times \exp(w) & \text{if } x > 0 \\ 0 & \text{otherwise} \end{cases}.$$

Consequently, the ExU units cannot learn the negative range of x because the back-propagation gradients are zero as $ReLU(x \times \exp(w))$ is always zero when $x \leq 0$.

In addition, we can suppose activation functions other than the ReLU. ExU units are also limited to other activation functions, as shown below. The w with an exponential function always greater than zero is as follows:

$$\forall w \in \mathbb{R} : \exp(w) > 0.$$

Therefore, the state of a linear transformation of an ExU unit is as follows:

$$\begin{cases} x \times \exp(w) \geq 0 & \text{if } x \geq 0 \\ x \times \exp(w) < 0 & \text{if } x < 0 \end{cases}.$$

When using ExU units, positive input x always has a positive effect, and negative input x always has a negative effect. \square

| | # samples | # features | positive rate | task |
|--------------------|-----------|------------|---------------|----------------|
| California Housing | 20,640 | 8 | - | regression |
| Insurance | 1,338 | 6 | - | regression |
| House Prices | 1,460 | 60 | - | regression |
| Bikeshare | 17,389 | 16 | - | regression |
| Year | 515,345 | 90 | - | regression |
| FICO | 10,459 | 23 | 0.478 | classification |
| Credit | 284,807 | 29 | 0.002 | classification |
| Support2 | 9,105 | 29 | 0.259 | classification |
| MIMIC III | 27,348 | 57 | 0.098 | classification |
| MIMIC IV | 451,608 | 8 | 0.018 | classification |
| COMPAS | 11,742 | 4 | 0.437 | classification |
| Click | 1M | 11 | 0.500 | classification |

Table 7: Datasets statistics

Datasets

We use the following 12 public datasets for our experiments:

- The California Housing dataset contains the 1990 California census information. The goal of this dataset is to predict the median values of houses in given California districts. <https://www.kaggle.com/datasets/camnugent/california-housing-prices>
- The Insurance dataset contains personal health information. The goal of this dataset is to predict individual medical costs billed by health insurance. <https://www.kaggle.com/datasets/mirichoi0218/insurance>
- The House Prices dataset contains housing information such as location and the total number of rooms. The goal of this dataset is to predict the sale prices of each house. <https://www.kaggle.com/competitions/house-prices-advanced-regression-techniques>
- The Bikeshare dataset contains the counts of rental bikes with the corresponding weather and seasonal features. <https://archive.ics.uci.edu/ml/datasets/bike+sharing+dataset>
- The Year dataset contains the features of songs ranging from 1922 to 2011. The goal of this dataset is to predict the release year of a song. <https://archive.ics.uci.edu/ml/datasets/yearpredictionmsd>
- The FICO dataset contains information from customers who requested credit lines. The goal of this dataset is to predict whether consumers who opened credit accounts have been past due for more than 90 days in the last 24 months. <https://community.fico.com/s/explainable-machine-learning-challenge>
- The Credit dataset contains completely de-identified features. The goal of this dataset is to detect credit fraud. Please see the original work (Dal Pozzolo 2015).
- The Support2 dataset contains patients information from study to understand prognoses preferences outcomes and risks of treatment. <https://biostat.app.vumc.org/wiki/Main/SupportDesc>
- The MIMIC III and MIMIC IV datasets are large-scale datasets containing a variety of hospital information, such as hospitalization and prescription information. Although there are many sub-tasks in this dataset, we focus on mortality prediction (Johnson et al. 2016, 2021).

- The COMPAS dataset contains personal and criminal information. The goal of this dataset is to predict whether the criminal risks are low or high. We set the target value to 0 if *text_score* is *Low* and 1 if *text_score* is *Medium* or *High* as same as the original work. <https://github.com/propublica/compas-analysis>
- The Click dataset contains advertising information. The goal of this dataset is to predict whether a user clicks an ad or not. We extracted positive and negative samples 500K as same as the previous work, respectively (Popov, Morozov, and Babenko 2019). <https://www.kaggle.com/c/kddcup2012-track2>

Preprocessing

For categorical features, we do ordinary encoding to reduce memory usage. For continuous features, we do standard scaling with mean and standard deviation. Then we do quantile transformation for all features. When fitting quantile transformation we add small gaussian noise. Adding noise is crucial to have mean and standard deviation close to 0 and 1, respectively (Chang, Caruana, and Goldenberg 2022).

Experimental Setup

We conducted experiments to demonstrate the effectiveness of the HONAM. The specifications of the experimental machine is Intel i7-8700 CPU, NVIDIA GeForce RTX 3090 TI GPU, and 64 GB RAM.

Dataset Split

For the California Housing, Insurance, House Prices, Bike-share, FICO, Credit, Support2, MIMIC, and COMPAS datasets, we randomly split training/validation/test sets into 60%/20%/20% ratio with 5 random seeds. For Year and Click datasets, we use training/validation/test sets provided by the previous work (Popov, Morozov, and Babenko 2019).

Hyperparameters

We use linear/logistic regression, CrossNet (Wang et al. 2017), XGBoost (Chen and Guestrin 2016), MLP, EBM (Nori et al. 2019), NAM (Agarwal et al. 2020), NodeGAM (Chang, Caruana, and Goldenberg 2022), NodeGA²M, and HONAM as experimental methods. All models, except XGBoost and EBM, is implemented using PyTorch. For MLP, NAM, and HONAM, the number of hidden layers is set to 3, the numbers of hidden units are set to [32, 64, 32], and LeakyReLU is used as the activation function. The number of units in CrossNet is set to 32. All PyTorch models are trained for 1000 epochs with the learning rate 0.001, and the batch size is used as the number of data samples divided by 100 to reduce the training time. The best validation model is selected for the test. For NodeGAM and NodeGA²M, we use the default hyperparameters provided by (Chang, Caruana, and Goldenberg 2022). We use the open-source version of XGBoost and EBM. For XGBoost, the number of boosting rounds is set to 1000 to ensure convergence, and eta is set to 0.3. For EBM, the number of boosting round is set to 20000 to ensure convergence, inner bags and outer bags are set to 8, and learning rate is set to 0.01 All models are trained with

5 random seeds, and we report mean scores and standard deviations.

Evaluation Metrics

The mean squared error and root mean squared error are representative evaluation metrics for regression. Still, because they are not scaled, it cannot be easy to evaluate whether the model really works well. Therefore, we used the R-squared score, which is a scaled evaluation metric. However, R-squared score relies only on mean squared error. To evaluate the regression models from a different perspective, we suggest R-absolute score, a novel scaled regression metric that relies on the mean absolute error. The R-absolute score is defined as follows:

$$R\text{-absolute} = \frac{\sum_{i=1}^N |y_i - \hat{y}_i|}{\sum_{i=1}^N |y_i - \bar{y}|}, \quad (16)$$

where N is the number of data samples. R-squared and R-absolute scores are used as evaluation metrics for regression tasks, and AUROC and AUPRC are used as evaluation metrics for classification tasks.

Feature Interaction Ablation Study

We conduct feature interaction ablation study. Table 8 and Table 9 show the predictive performances of CrossNet and HONAM. *HONAM** indicates HONAM with CrossNet, and *HONAM* indicates HONAM with the proposed feature interaction method. We use 2nd-, 3rd-, and 4th-order CrossNet and HONAM for the ablation study. The predictive performances are improved as the interaction order is increased. However, significant performance improvements do not appear in some datasets. Perhaps it is because they are vulnerable to overfitting, or there are no feature interactions in the dataset. Nevertheless, we believe that high-order interactions are important from interpretability perspective because they allow the discovery of co-relationships between different features.

Learning Sharp Jumps

Synthetic Dataset Generation

The synthetic classification dataset was generated as follows: We randomly sampled 100 points in [-1, 1] for the input x . We then randomly sampled p in [0.1, 0.9] and generated 100 labels (0 or 1) from a binomial distribution with probability p for each x . The synthetic classification dataset contained 10,000 samples. The shape function of the training model should fit the log odds of the probability p . Additionally, we generated a synthetic regression dataset for an additional experiment. The synthetic regression dataset was generated as follows: We randomly sampled 100 points in [-1, 1] for input x , and the corresponding target y was also sampled in [-1, 1]. The synthetic regression dataset contained 100 samples.

Learned Shape Plots on Synthetic Dataset

Figure 8 and Figure 9 show the shape plots learned by ExU, and ExpDive units on synthetic regression and classification datasets, respectively. Consistent with *Theorem 2*, the

| | California Housing | | Insurance | | House Prices | | Bikeshare | | Year | |
|----------------|------------------------------|------------------------------|------------------------------|------------------------------|------------------------------|------------------------------|------------------------------|------------------------------|------------------------------|------------------------------|
| | R-squared | R-absolute | R-squared | R-absolute | R-squared | R-absolute | R-squared | R-absolute | R-squared | R-absolute |
| CrossNet (t=2) | 0.717 (± 0.001) | 0.525 (± 0.001) | 0.860 (± 0.005) | 0.688 (± 0.020) | 0.885 (± 0.011) | 0.683 (± 0.003) | 0.498 (± 0.008) | 0.316 (± 0.009) | 0.310 (± 0.001) | 0.211 (± 0.001) |
| CrossNet (t=3) | 0.739 (± 0.004) | 0.549 (± 0.004) | 0.854 (± 0.007) | 0.691 (± 0.020) | 0.903 (± 0.007) | 0.720 (± 0.007) | 0.590 (± 0.017) | 0.403 (± 0.009) | 0.324 (± 0.001) | 0.228 (± 0.002) |
| CrossNet (t=4) | 0.741 (± 0.007) | 0.562 (± 0.006) | 0.855 (± 0.010) | 0.690 (± 0.007) | 0.903 (± 0.007) | 0.718 (± 0.008) | 0.645 (± 0.013) | 0.453 (± 0.011) | 0.327 (± 0.002) | 0.236 (± 0.002) |
| HONAM* (t=2) | 0.807 (± 0.004) | 0.621 (± 0.004) | 0.880 (± 0.001) | 0.744 (± 0.003) | 0.900 (± 0.018) | 0.725 (± 0.017) | 0.920 (± 0.004) | 0.752 (± 0.008) | 0.320 (± 0.003) | 0.224 (± 0.003) |
| HONAM* (t=3) | 0.810 (± 0.008) | 0.629 (± 0.009) | 0.882 (± 0.001) | 0.743 (± 0.005) | 0.905 (± 0.020) | 0.730 (± 0.022) | 0.945 (± 0.005) | 0.806 (± 0.010) | 0.329 (± 0.004) | 0.235 (± 0.006) |
| HONAM* (t=4) | 0.804 (± 0.005) | 0.624 (± 0.004) | 0.881 (± 0.002) | 0.741 (± 0.006) | 0.904 (± 0.025) | 0.728 (± 0.034) | 0.949 (± 0.003) | 0.816 (± 0.004) | 0.331 (± 0.005) | 0.243 (± 0.008) |
| HONAM (t=2) | 0.810 (± 0.003) | 0.626 (± 0.003) | 0.882 (± 0.002) | 0.742 (± 0.012) | 0.900 (± 0.011) | 0.721 (± 0.009) | 0.925 (± 0.004) | 0.760 (± 0.006) | 0.320 (± 0.002) | 0.226 (± 0.004) |
| HONAM (t=3) | 0.804 (± 0.004) | 0.623 (± 0.001) | 0.881 (± 0.002) | 0.741 (± 0.004) | 0.904 (± 0.016) | 0.728 (± 0.004) | 0.952 (± 0.003) | 0.817 (± 0.004) | 0.327 (± 0.005) | 0.237 (± 0.006) |
| HONAM (t=4) | 0.805 (± 0.003) | 0.619 (± 0.004) | 0.881 (± 0.002) | 0.740 (± 0.005) | 0.909 (± 0.015) | 0.735 (± 0.011) | 0.952 (± 0.003) | 0.819 (± 0.004) | 0.326 (± 0.002) | 0.237 (± 0.005) |

Table 8: Interaction Ablation Study on Regression Tasks

| | FICO | | Credit | | Support2 | | MIMIC III | | Click | |
|----------------|------------------------------|------------------------------|------------------------------|------------------------------|------------------------------|------------------------------|------------------------------|------------------------------|------------------------------|------------------------------|
| | AUROC | AUPRC | AUROC | AUPRC | AUROC | AUPRC | AUROC | AUPRC | AUROC | AUPRC |
| CrossNet (t=2) | 0.770 (± 0.002) | 0.752 (± 0.004) | 0.964 (± 0.024) | 0.810 (± 0.038) | 0.803 (± 0.009) | 0.612 (± 0.013) | 0.787 (± 0.005) | 0.343 (± 0.022) | 0.619 (± 0.001) | 0.625 (± 0.001) |
| CrossNet (t=3) | 0.772 (± 0.001) | 0.754 (± 0.002) | 0.969 (± 0.016) | 0.824 (± 0.042) | 0.794 (± 0.013) | 0.601 (± 0.019) | 0.768 (± 0.010) | 0.341 (± 0.022) | 0.616 (± 0.003) | 0.616 (± 0.003) |
| CrossNet (t=4) | 0.772 (± 0.002) | 0.755 (± 0.003) | 0.965 (± 0.024) | 0.838 (± 0.033) | 0.798 (± 0.007) | 0.605 (± 0.010) | 0.775 (± 0.009) | 0.342 (± 0.027) | 0.617 (± 0.003) | 0.619 (± 0.003) |
| HONAM* (t=2) | 0.783 (± 0.003) | 0.761 (± 0.005) | 0.982 (± 0.009) | 0.842 (± 0.024) | 0.819 (± 0.009) | 0.633 (± 0.011) | 0.825 (± 0.003) | 0.395 (± 0.023) | 0.667 (± 0.004) | 0.663 (± 0.003) |
| HONAM* (t=3) | 0.781 (± 0.002) | 0.759 (± 0.003) | 0.987 (± 0.006) | 0.853 (± 0.031) | 0.819 (± 0.008) | 0.632 (± 0.014) | 0.824 (± 0.002) | 0.388 (± 0.023) | 0.667 (± 0.003) | 0.656 (± 0.003) |
| HONAM* (t=4) | 0.780 (± 0.001) | 0.758 (± 0.002) | 0.982 (± 0.017) | 0.851 (± 0.061) | 0.819 (± 0.010) | 0.633 (± 0.012) | 0.822 (± 0.005) | 0.386 (± 0.022) | 0.664 (± 0.006) | 0.657 (± 0.005) |
| HONAM (t=2) | 0.782 (± 0.002) | 0.760 (± 0.004) | 0.981 (± 0.012) | 0.838 (± 0.026) | 0.823 (± 0.011) | 0.640 (± 0.009) | 0.826 (± 0.005) | 0.399 (± 0.024) | 0.670 (± 0.002) | 0.664 (± 0.003) |
| HONAM (t=3) | 0.782 (± 0.002) | 0.760 (± 0.004) | 0.981 (± 0.009) | 0.843 (± 0.031) | 0.820 (± 0.010) | 0.637 (± 0.014) | 0.826 (± 0.004) | 0.397 (± 0.022) | 0.669 (± 0.002) | 0.663 (± 0.002) |
| HONAM (t=4) | 0.780 (± 0.002) | 0.758 (± 0.004) | 0.983 (± 0.009) | 0.840 (± 0.035) | 0.819 (± 0.010) | 0.636 (± 0.013) | 0.824 (± 0.004) | 0.390 (± 0.019) | 0.668 (± 0.005) | 0.662 (± 0.005) |

Table 9: Interaction Ablation Study on Classification Tasks

ExU unit cannot learn well in the range of negative x on both datasets. Our ExpDive unit learned the sharpest function on both datasets. In addition, we found that the joint learning models can learn extremely sharp shape functions. Figure 10 and 11 show the shape plots learned by the joint learning model with 100 ExU, and ExpDive units, respectively. Since the joint learning models have high capacity and sub-networks cooperate to predict a single data point, they can learn extremely sharp shape functions. Therefore, the ExU unit works well in the negative range of x .

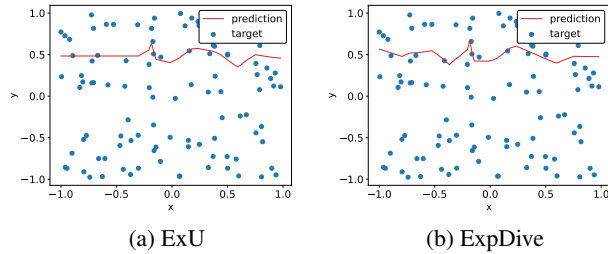


Figure 8: Learned shape functions of different units with single feature network on synthetic regression task

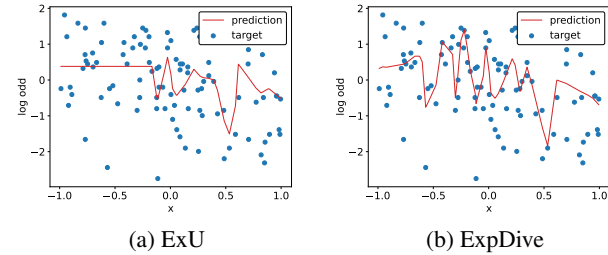


Figure 9: Learned shape functions of different units with single feature network on synthetic classification task

Interpreting HONAM

Extracting Feature Shape Plots

We can acquire direct feature contribution values via forward propagation of HONAM. For example, we refer the representation vectors of each input feature x_1, x_2, \dots, x_m computed by the feature networks as r_1, r_2, \dots, r_m , where m is the number of features. To obtain 1st-order interpretation, the contribution value of feature i is computed by $r_i \times w_{0,k}$, where w is the output matrix and k is the

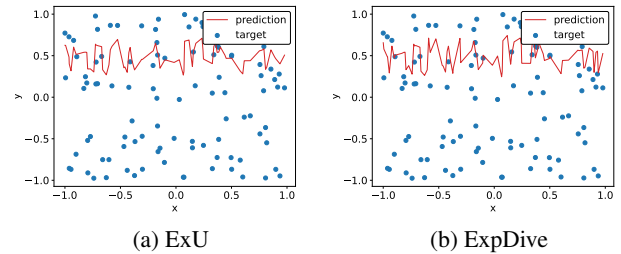


Figure 10: Learned shape functions of different units with multiple feature networks on synthetic regression task

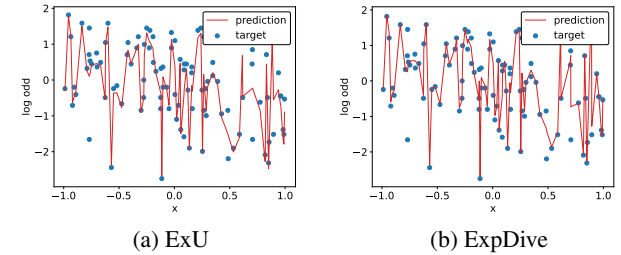


Figure 11: Learned shape functions of different units with multiple feature networks on synthetic classification task

size of the representation vector. Similarly, the contribution value of 2^{nd} -order feature $(x_i * x_j)$ can be computed as $(r_i * r_j) \times w_{k:2*k}$. The purification, as in NodeGAM, is not needed because, 1) in our HONAM, a feature has only one corresponding representation vector, 2) this representation vector is directly connected to the output layer, and 3) our feature interaction method does not learn multi-terms polynomials. For example, our interaction method only learns interactions between different features such as $x_1 \times x_2$ or $x_1 \times x_3 \times x_7$, it does not learn multi-terms polynomials such as $x_1x_2 + x_2$ or $x_2x_3 + x_2$.

Visualization of Feature Contributions

Figure 12 and 13 show the shape plots of the 1st-order and 2nd-order features on the CA Housing dataset. Figure 14 and 15 show the shape plots of the 1st-order and 2nd-order features on the FICO Housing dataset.

We can get some insights from the figures. First, HONAM can learn soft (or smooth) nonlinear functions because it uses neural networks. Because the conventional GAM can only learn linear functions, its expressive power is limited. In addition, because tree-based models, such as boosting trees, can only learn discretized functions, they require a massive number of trees to learn smooth-looking functions. Therefore, it is difficult to extend various settings, such as multi-label or multi-class learning (Agarwal et al. 2020), and their explanations are difficult to understand. Second, HONAM can learn sharp jumps. In the California Housing dataset, HONAM learned a few sharp jumps. We believe that our ExpDive unit is more effective in a field where sharp jumps frequently occur, such as in stock price predictions. Third, we can view the relationships between features via HONAM. In other words, HONAM provides more detailed interpretations than NAM and other interpretable methods.

Discussion

In this section, we would like to discuss the limitations of interpretable machine learning, NAM-family methods, and HONAM.

Interpretable machine learning methods allow us to understand their decision-making processes. However, it is impossible to determine why certain features are important and why certain features have positive or negative influences. For example, in Figure 4a, *ExternalRistEstimate* has the greatest influence. In other words, the model determined that this feature was the most important; however, why? Human assistance is required to understand this. Therefore, interpretable machine learning still requires human effort, and we take care when interpreting the results of a model.

The NAM family of methods requires different feature networks corresponding to each feature. This strategy creates an interpretable model but is time-consuming. Fast training and inference are important in real-world systems. Therefore, we need an interpretable method that is faster than the NAM.

HONAM uses all feature combinations to model interactions. However, modeling all interactions slows down the execution time and can reduce the predictive performance

because some interactions may be noisy (Cheng, Shen, and Huang 2020). If HONAM can adaptively learn feature interactions, it may have higher predictive performance, interpretability, and faster execution time.

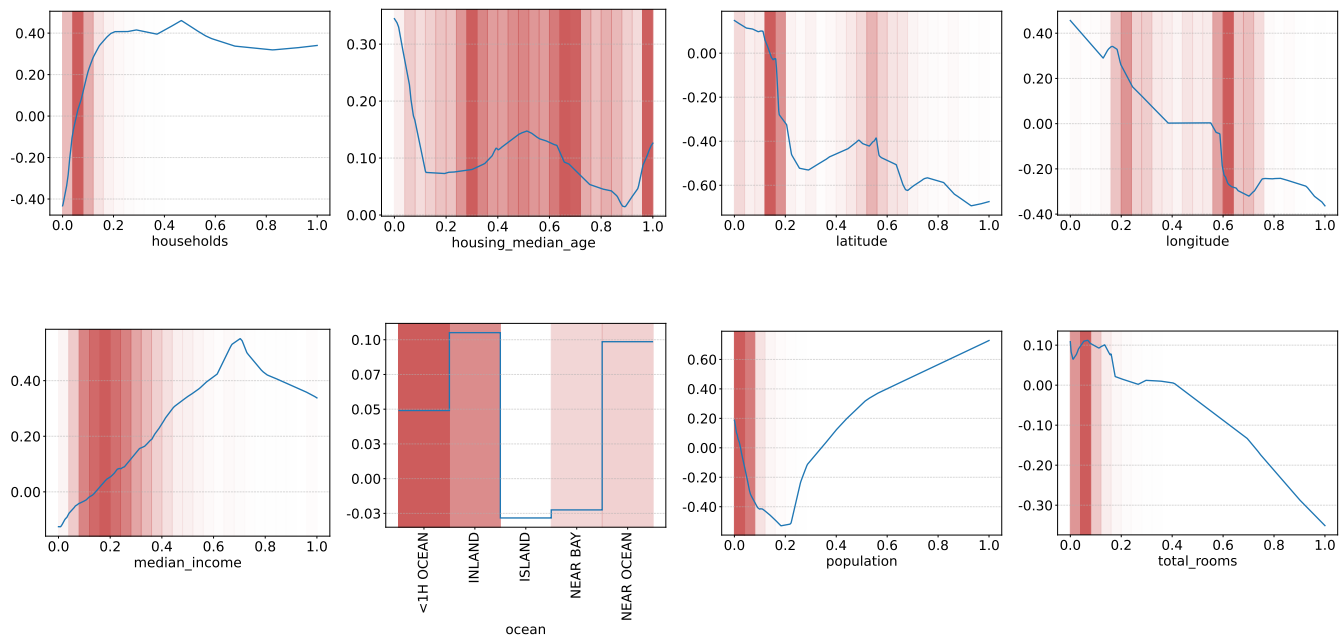


Figure 12: Learned shape plots of 1st-order features on the CA Housing dataset

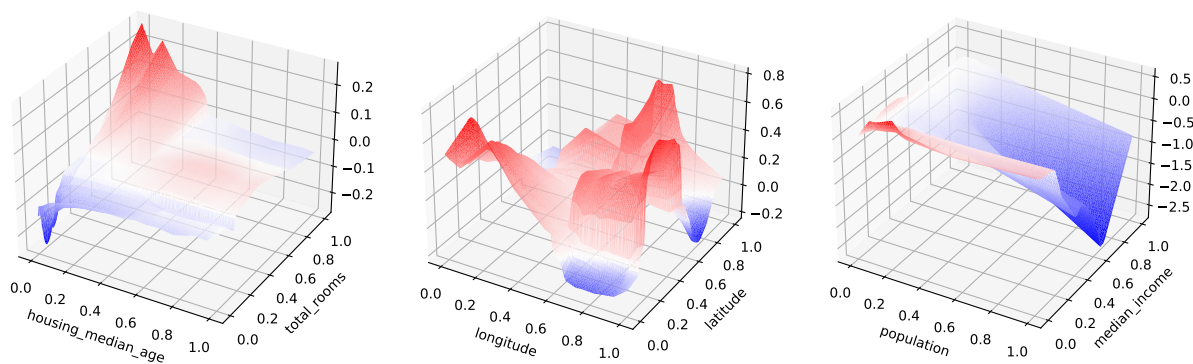


Figure 13: Learned shape plots of 2nd-order features on the CA Housing dataset

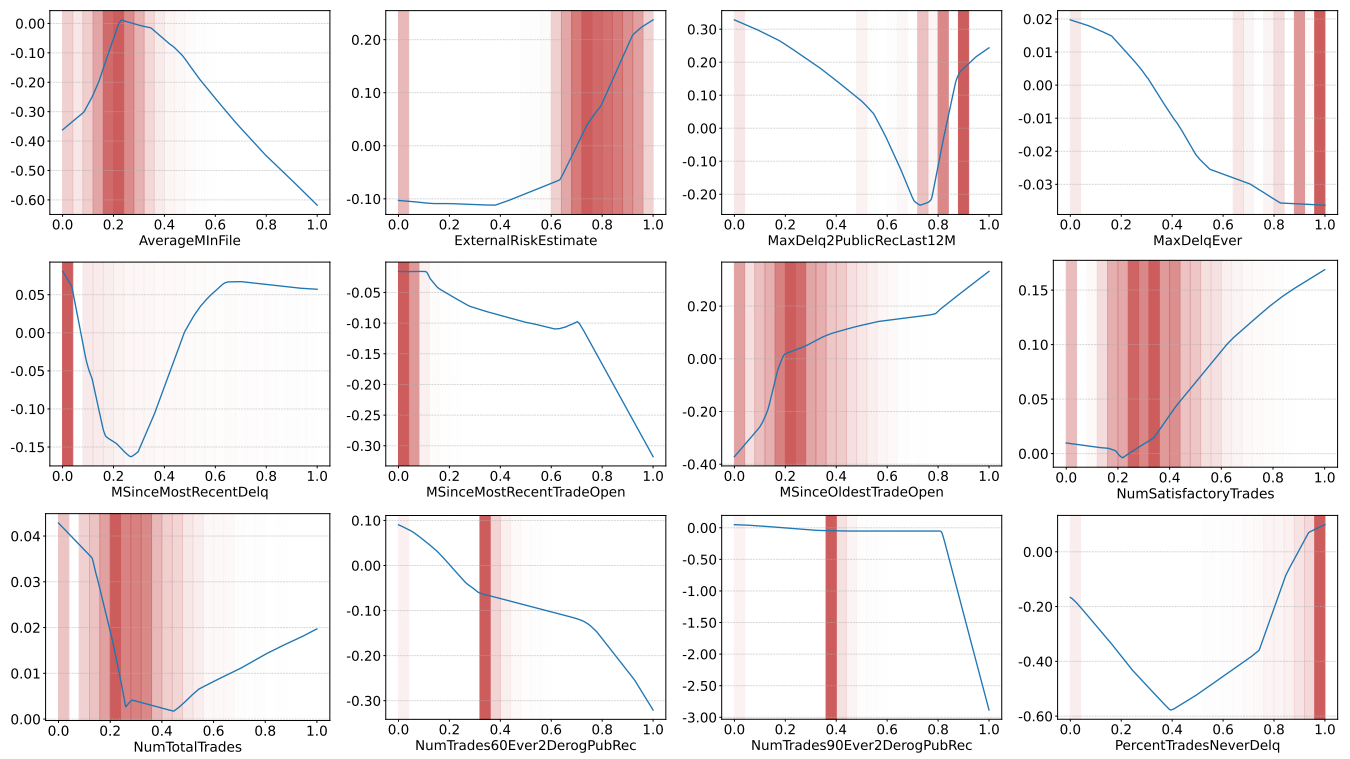


Figure 14: Learned shape plots of 1st-order features on the FICO dataset

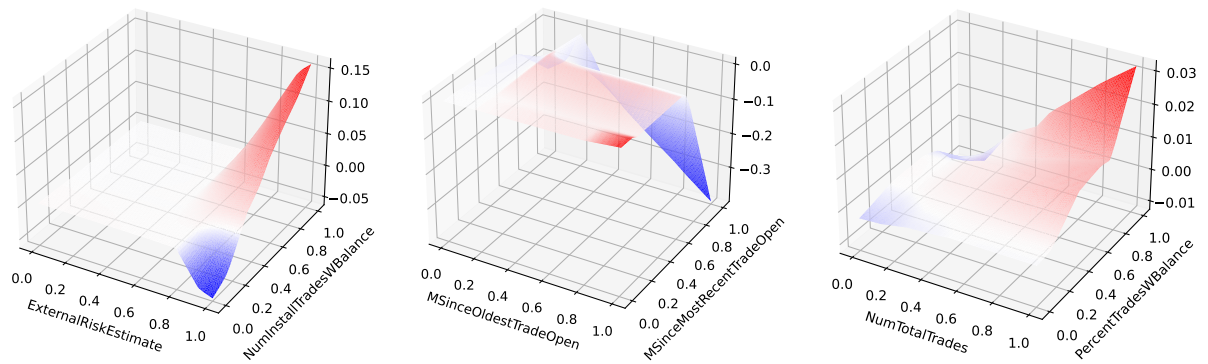


Figure 15: Learned shape plots of 2nd-order features on the FICO dataset

Algorithm 1: Forward propagation of Feature Network

Input:input features x **Parameter:**number of layers l trainable weights w_1, w_2, \dots, w_l trainable biases b_1, b_2, \dots, b_l 1: **for** $i \leftarrow 1$ **to** l **do**2: $x \leftarrow xw_i + b_i$ 3: $x \leftarrow \sigma(x)$ 4: **end for**5: **return** x ▷ linear transformation of x ▷ activation function

Algorithm 2: Forward propagation of HONAM

Input:input features x **Parameter:**number of features m order of interaction t feature networks corresponding to each feature f_1, f_2, \dots, f_m trainable weight w trainable bias b 1: **for** $i \leftarrow 1$ **to** m **do**2: $repr_i \leftarrow f(x_i)$ 3: **end for**

▷ run feature network, see Algorithm 1

4: $fi_0, pfi_0 \leftarrow 1, 1$ 5: $fi_1, pfi_1 \leftarrow \sum_{i=1}^m repr_i, \sum_{i=1}^m repr_i$

▷ init interactions

▷ sum of 1st-order interactions6: **for** $i \leftarrow 2$ **to** t **do**7: $sign \leftarrow 1$ 8: $pfi_i \leftarrow \sum_{k=1}^m repr_k^i$ 9: $fi_i \leftarrow 0$ 10: **for** $j \leftarrow 1$ **to** i **do**11: $fi_i \leftarrow fi_i + sign \times pfi_j \times fi_{i-j}$ 12: $sign = -sign$ 13: **end for**14: $fi_i \leftarrow fi_i / i$ 15: **end for**

▷ high-order interaction modeling

16: $pred \leftarrow fi_{1:m}w + b$

▷ prediction

17: **return** $pred$
